BIOCHEMICAL PHARMACOLOGY 76 (2008) 169–178

available at www.sciencedirect.com

ScienceDirect

journal homepage: www.elsevier.com/locate/biochempharm

Validating the mitotic kinesin Eg5 as a therapeutic target in pancreatic cancer cells and tumor xenografts using a specific inhibitor

*Min Liu, Haiyang Yu, Lihong Huo, Jianchao Liu, Minggang Li *, Jun Zhou **

Department of Genetics and Cell Biology, College of Life Sciences, Nankai University, 94 Weijin Road, Tianjin 300071, China

ARTICLE INFO

Article history:
Received 10 March 2008
Accepted 15 April 2008

Keywords:
Pancreatic cancer
Eg5 inhibitor
Spindle checkpoint
Apoptosis
Tumor xenograft

ABSTRACT

Pancreatic cancer is a devastating disease with a high mortality rate. Treatment of this malignancy remains a big challenge in oncology, and none of the currently available chemotherapeutic agents has a remarkable impact on improving patient survival. Consequently, it is important to explore new targets and find effective drugs for the management of this disease. Here we report that inhibition of the mitotic kinesin Eg5 by a pharmacological compound effectively prevents the proliferation of pancreatic cancer cells by halting mitotic progression, resulting in robust apoptosis. The mitotic arrest induced by this agent is attributed to its interference with spindle formation and activation of the spindle checkpoint. Impairment of the spindle checkpoint significantly compromises both mitotic arrest and apoptosis induced by the Eg5 inhibitor, suggesting the importance of the spindle checkpoint in monitoring Eg5 inhibitor sensitivity. Furthermore, treatment of nude mice bearing tumor xenografts of human pancreatic cancer results in pronounced tumor regression by triggering apoptosis. These data thus indicate Eg5 as a potential target for pancreatic cancer treatment.

1. Introduction

Pancreatic cancer is the fourth leading cause of cancer death in the world. The median survival is less than a year, and the 5-year survival rate is less than 5%, the lowest among all major cancers [1]. Pancreatic cancer is usually diagnosed at the advanced stage due to its insidious progression and rapid dissemination to other organs [2,3]. By the time symptoms appear, the majority of patients present with locally advanced or metastatic disease that is surgically inoperable. Even for patients who have undergone curative resection, most of them will recur within 2 years of surgical operation and will die of this malignancy. The devastating feature of pancreatic cancer is primarily due to its resistance to conventional chemotherapeutic agents in addition to its enormous aggressive biology [2,3]. Treatment options for this disease are very limited. Systemic chemotherapy has not been quite successful, although the use of gemcitabine, the standard drug for advanced pancreatic cancer, results in modest clinical benefit in a subset of patients [4].

There has been a worldwide effort in the past few years to evaluate the effect of many other chemotherapeutics in combination with gemcitabine for the treatment of pancreatic cancer [5]. Unfortunately, the combinations fail to significantly improve the symptoms and do not show an obvious survival benefit compared with gemcitabine alone [4]. Thus, there is an urgent need to identify efficacious drugs, especially for the majority of patients who suffer from locally advanced or metastatic disease, for which no curative therapies exist to date. In the present study, dimethylenastron, a specific

* *Corresponding authors*. Tel.: +86 22 2350 4946; fax: +86 22 2350 4946.
E-mail addresses: mgl@nankai.edu.cn (M. Li), junzhou@nankai.edu.cn (J. Zhou).
0006-2952/$ – see front matter
doi:10.1016/j.bcp.2008.04.018

inhibitor of the mitotic kinesin Eg5 [6], was found to effectively inhibit the proliferation of pancreatic cancer cells by blocking cell-cycle progression at mitosis, leading to apoptotic cell death. The spindle checkpoint, which functions to ensure accurate chromosome segregation in mitosis [7,8], was found to regulate the Eg5 inhibitor sensitivity in pancreatic cancer cells. In addition, the Eg5 inhibitor exhibited potent activity in mice bearing tumor xenografts of human pancreatic cancer. These results suggest that Eg5 may be an effective target for chemotherapeutic management of pancreatic cancer.

2. Materials and methods

2.1. Materials

7,7-Dimethyl-4-(3-hydroxyphenyl)-5-oxo-3,4,5,6,7,8-hexahydroquinazolin-2(1*H*)-thione (known as dimethylenastron) was prepared as described [6]. In brief, 3-hydroxybenzaldehyde, 5,5-dimethyl-1,3-cyclohexanedione, and thiourea were mixed with polyphosphate ester in a glass beaker and irradiated in a microwave oven. Ethanol and water were then added to the mixture, and the solid was dissolved in an ultrasonic bath. The resulting solution was poured into stirred ice-cold water. The precipitated crude product was filtered off and dried in vacuum. The product was subsequently purified by flash-chromatography (purity $\geq$95%). HR22C16 and monastrol were purchased from EMD Chemicals (Gibbstown, NJ, US). Taxol, doxorubicin, sulforhodamine B, 3-(4,5-dimethyl-2-thiazolyl)-2,5-diphenyl-2*H*-tetrazolium bromide (MTT), 4′-6-diamidino-2-phenylindole (DAPI), propidium iodide, and a mouse monoclonal antibody against α-tubulin were from Sigma–Aldrich (St. Louis, MO, US). Rabbit polyclonal antibodies against Mad2 and BubR1 were obtained from Abcam. Horseradish peroxidase-conjugated anti-rabbit and anti-mouse secondary antibodies were purchased from Amersham Biosciences. Fluorescein-conjugated anti-mouse and rhodamine-conjugated anti-rabbit secondary antibodies were from Jackson ImmunoResearch Laboratories.

2.2. Cells and adenoviruses

EPP85, BxPC3, CFPAC1, and AsPC1 human pancreatic cancer cells and RPMI8226 human multiple myeloma cells were cultured in RPMI 1640 medium supplemented with 2 mM L-glutamine and 10% fetal bovine serum at 37 °C in a humidified atmosphere with 5% CO_2. Adenoviruses encoding Mad2, BubR1, and dominant-negative Mad2 and BubR1 were prepared and amplified in low passage human embryonic kidney 293 cells as described previously [9,10]. Adenovirus titers were determined with an adenovirus titer kit (BD Biosciences).

2.3. Small interfering RNAs (siRNAs)

Mad2, BubR1, and luciferase siRNAs (21-nucleotide duplexes) were designed to target Mad2 sequence 5′-ACCTTTACTCGAGTGCAGA-3′, BubR1 sequence 5′-CAATACTCTTCAGCAGCAG-3′, and luciferase sequence 5′-CGTACGCGGAATACTTCGA-3′, respectively. The siRNAs were synthesized by Dharmacon and transfected to cells with the lipofectamine 2000 reagent following the manufacturer's instruction (Invitrogen).

2.4. In vitro cell proliferation assay

Cells grown in 96-well plates were treated with gradient concentrations of dimethylenastron for 48 h. Sulforhodamine B and MTT assays were then performed as described previously [11]. The percentage of cell proliferation as a function of drug concentration was plotted to determine IC_{50}, which stands for the drug concentration needed to prevent cell proliferation by 50%.

2.5. Flow cytometry

Flow cytometric evaluation of cellular DNA content was performed as described [12]. Briefly, 2×10^6 cells were collected, washed twice with ice-cold phosphate-buffered saline (PBS), and fixed in 70% ethanol for 24 h. Cells were washed again with PBS and incubated with propidium iodide (20 μg/ml)/RNaseA (20 μg/ml) in PBS for 30 min in the dark. Samples were analyzed on a BD FACSCalibur flow cytometer.

2.6. Fluorescence microscopy

To visualize microtubules, cells grown on glass coverslips were fixed with cold (−20 °C) methanol for 5 min and then washed with PBS for 5 min. Nonspecific sites were blocked by incubating with 2% BSA in PBS for 15 min. Cells were incubated with mouse monoclonal anti-α-tubulin antibody for 2 h and then fluorescein-conjugated anti-mouse secondary antibody for 1 h, followed by staining with DAPI for 5 min as described [13]. Coverslips were mounted with 90% glycerol in PBS and examined with an Olympus fluorescence microscope. To visualize the spindle checkpoint proteins Mad2, Bub1, and BubR1, cells grown on glass coverslips were fixed with 1% paraformaldehyde/PBS for 20 min at room temperature. Coverslips were then washed with PBS for 5 min, permeabilized with 0.2% Triton X-100/PBS for 2 min, and washed for another 5 min with PBS before they were processed for incubation with primary and secondary antibodies, stained with DAPI, and examined microscopically.

2.7. Western blot analysis

Proteins were resolved by polyacrylamide gel electrophoresis and transferred onto polyvinylidene difluoride membranes (Millipore). The membranes were blocked in Tris-buffered saline containing 0.2% Tween 20 and 5% fat-free dry milk and incubated first with primary antibodies and then with horseradish peroxidase-conjugated secondary antibodies. Specific proteins were visualized with enhanced chemiluminescence detection reagent according to the manufacturer's instructions (Pierce Biotechnology).

2.8. MPM2 antibody staining

Cells (2×10^6) were collected and fixed with 70% ethanol. Cells were then treated with the blocking solution (PBS containing 0.2%, w/v saponin and 0.2% BSA) for 1 h, followed by incubation with the MPM2 mouse monoclonal antibody (Upstate Technology) in the blocking solution for 1 h. Cells were then incubated with Alexa 488-conjugated anti-mouse secondary antibody

(Molecular Probes) for 1 h, and the percentage of MPM2-positive cells was quantified by flow cytometry.

2.9. Annexin V staining

The annexin V staining assay was performed by using the annexin V apoptosis detection kit following the manufacturer's protocol (Pharmingen). Briefly, cells were washed with PBS and then resuspended in the binding buffer (10 mM HEPES, pH 7.4, 140 mM NaCl, 2.5 mM $CaCl_2$). Cells were incubated with fluorescein-conjugated annexin V for 15 min at room temperature in the dark. The binding buffer was then added and cells were analyzed by flow cytometry.

2.10. Measurement of caspase-3 activity

Cells were incubated with 0.4 or 1 μM dimethylenastron or vehicle control for 0, 24, 48, or 72 h. Caspase-3 activity was examined by measuring the luminescence resulting from the cleavage of Z-DEVD-aminoluciferin (Promega). The luminescent signal, which is directly proportional to the level of caspase-3 activity, was measured with a luminescence plate reader.

2.11. Animal experiment

Eight-week-old female BALB/c athymic (nu/nu) nude mice were injected subcutaneously with 2×10^6 EPP85 cells per mouse. Treatment was initiated 8 days later when tumors were palpable and measurable (about 100 mm^3). Three axes of tumors were measured every 2 days with vernier calipers, and tumor volume was calculated as $1/2 \times \text{length} \times \text{width}^2$ in mm^3. Tumor-bearing mice were randomly grouped (8 mice/group) and were treated intravenously with 10, 20, or 40 mg/kg dimethylenastron or equal volume of vehicle. Body weight was monitored every 2 days. At the end of experiment, tumors were formalin-fixed and paraffin-embedded.

2.12. Terminal deoxynucleotidyltransferase-mediated dUTP nick-end labeling (TUNEL) staining of tumor sections

For TUNEL staining of paraffin-embedded tumor sections, tumors were dewaxed at 60 °C for 15 min, washed in xylene, and then rehydrated through a graded series of ethanol and distilled water. The resulting sections were incubated with proteinase K for 20 min, incubated with the blocking solution

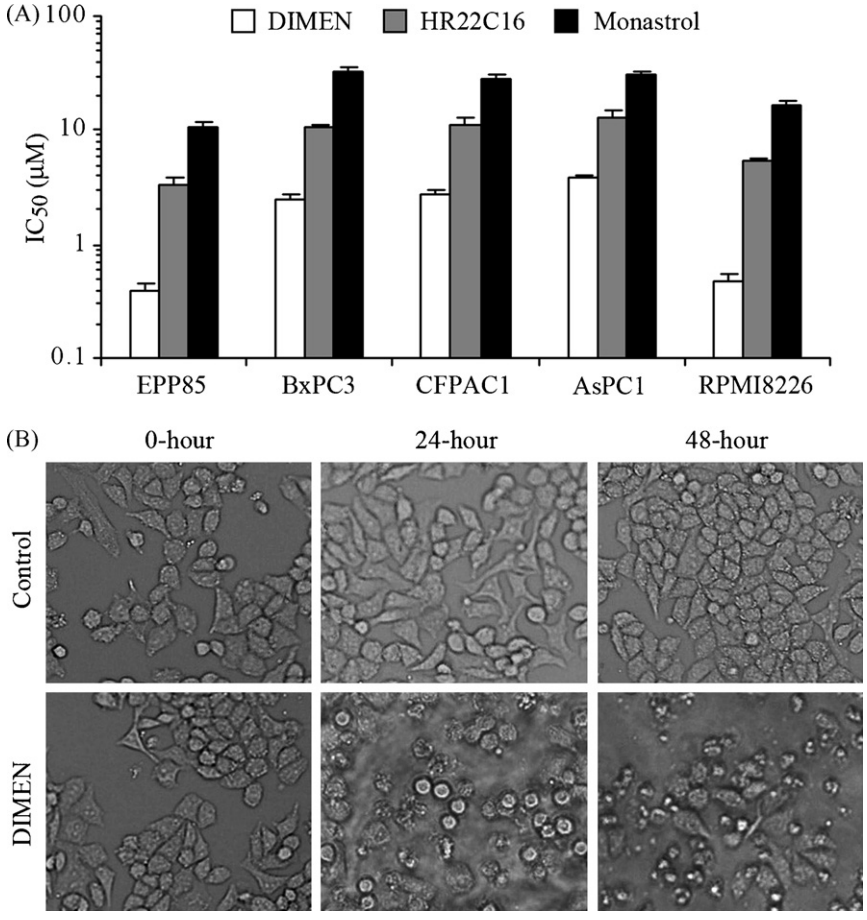

Fig. 1 – Inhibition of Eg5 activity prevents the proliferation of human pancreatic cancer cells. (A) EPP85, BxPC3, CFPAC1, and AsPC1 pancreatic cancer cells and RPMI8226 multiple myeloma cells were treated with varying concentrations of dimethylenastron (DIMEN), HR22C16, or monastrol for 48 h, and the drug concentrations needed for 50% inhibition of cell proliferation (IC_{50} values) were then determined by sulforhodamine B-based in vitro cell proliferation assay. The values and error bars shown in the graph represent the averages and standard deviations, respectively, of three independent experiments. (B) Phase contrast images of EPP85 cells treated with 0.4 μM dimethylenastron for 0, 24, or 48 h.

(0.3% H_2O_2 in methanol) for 30 min, and then incubated in the permeabilization solution (0.1% Triton X-100/0.1% sodium citrate) on ice for 2 min. The slides were incubated with TUNEL reaction mixture (Molecular Probes) for 1 h at 37 °C in a humidified chamber, incubated with streptavidin-horseradish peroxidase solution for 30 min, and then incubated with 3,3′-diaminobenzidine solution for 10 min.

3. Results

3.1. *Inhibition of Eg5 activity prevents the proliferation of human pancreatic cancer cells*

Inhibitors of the mitotic kinesin Eg5 represent a new generation of anti-cancer agents currently undergoing clinical evaluation [14]. To examine the therapeutic potential of targeting Eg5 in pancreatic cancer, EPP85, BxPC3, CFPAC1, and AsPC1 human pancreatic cancer cells were treated with gradient concentrations of the Eg5 inhibitors dimethylenastron, HR22C16, and monastrol. The extent of cell proliferation was measured by sulforhodamine B staining assay, which is based on the stoichiometric binding of the sulforhodamine B dye to all cellular protein components [15]. The IC_{50} values, which stand for the drug concentrations needed for 50% inhibition of cell proliferation, were then determined. RPMI8226 multiple myeloma cells were used as positive controls for the pancreatic cancer cells [12]. As shown in Fig. 1A, the Eg5 inhibitors effectively prevented the proliferation of RPMI8226 cells, with dimethylenastron showing the highest activity. Dimethylenastron also exhibited strikingly higher anti-proliferative activity than HR22C16 and monastrol for all the pancreatic cancer cell lines examined (Fig. 1A). In addition, we found that the EPP85 cell line was more sensitive to Eg5 inhibitor treatment than the other pancreatic cancer cell lines. Similar results were achieved using MTT-based in vitro cell proliferation assay (data not

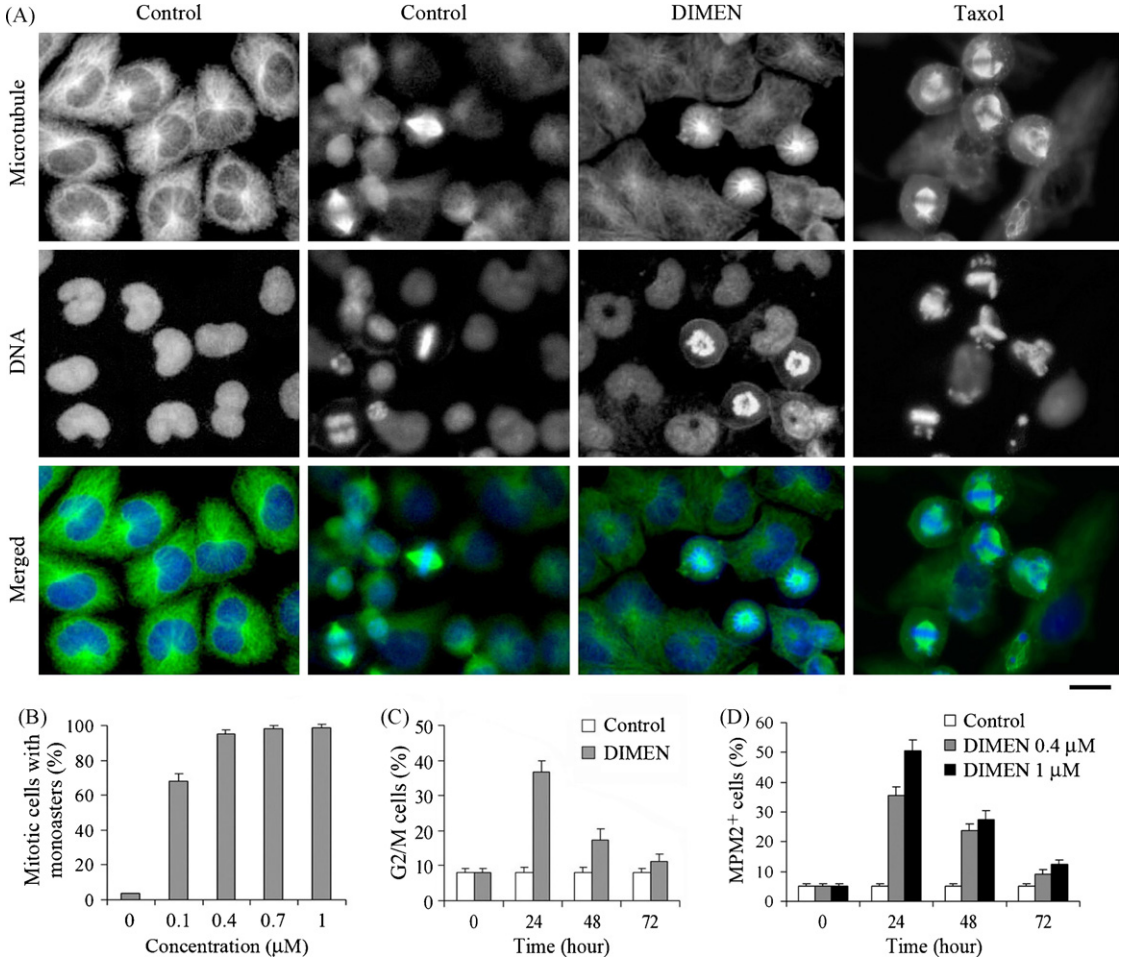

Fig. 2 – Dimethylenastron arrests cells at mitosis and interferes with bipolar spindle formation. (A) Immunofluorescence images of microtubules (green) and DNA (blue) in EPP85 cells treated for 24 h with 0.4 μM dimethylenastron, 5 nM taxol, or vehicle (control). The left control shows the morphology of interphase cells in vehicle-treated group, whereas the right control highlights the morphology of mitotic cells in vehicle-treated group. Bar, 10 μm. (B) Cells were treated for 24 h with 0, 0.1, 0.4, 0.7, or 1 μM dimethylenastron, and the percentage of mitotic cells with monoasters was quantified by immunofluorescence staining of cellular microtubules and DNA as in (A). (C) Cells were treated with 0.4 μM dimethylenastron or vehicle (control) for 0, 24, 48, or 72 h, and the percentage of G2/M phase cells was quantified by flow cytometric analysis of cellular DNA content. (D) Cells were treated with 0.4 or 1 μM dimethylenastron or vehicle (control) for 0, 24, 48, or 72 h, and the percentage of mitotic cells was quantified by MPM2 antibody staining assay.

shown). Therefore, we chose to use dimethylenastron and EPP85 cells in the following studies to further validate the potential of Eg5 as a therapeutic target against pancreatic cancer. Phase contrast microscopic analysis of cell morphology revealed that while EPP85 cells proliferated normally upon vehicle treatment, their proliferation was significantly impaired in the presence of dimethylenastron. Following drug exposure, cells turned round first (24-h treatment) and then appeared fragmented (48-h treatment) (Fig. 1B).

3.2. *Dimethylenastron arrests cells at mitosis and interferes with bipolar spindle formation*

We next investigated the molecular mechanisms underlying the anti-proliferative activity of dimethylenastron in pancreatic cancer cells. We first examined cellular microtubules and DNA in dimethylenastron-treated EPP85 cells by immunofluorescence microscopy. As shown in Fig. 2A, following a 24-h treatment with 0.4 μM dimethylenastron, many EPP85 cells were blocked at mitosis with condensed chromosomes. Strikingly, while normal mitotic cells have bipolar spindles and the majority of 5 nM taxol (a microtubule-binding drug)-arrested mitotic cells have multipolar spindles, dimethylenastron-arrested mitotic cells have monopolar spindles known as monoasters (Fig. 2A and B). Dimethylenastron-induced mitotic arrest was confirmed by flow cytometric analysis of cellular DNA content. As shown in Fig. 2C, dimethylenastron remarkably increased the fraction of G2/M phase cells, which have a duplicated complement (4N) of DNA, compared with the vehicle-treated group (Fig. 2C). The percentage of G2/M cells peaked at 24 h of drug treatment and then went down gradually (Fig. 2C). The mitotic arrest induced by dimethylenastron was further confirmed by measuring the proportion of cells stained by a mitosis-specific antibody, MPM2 [16] (Fig. 2D).

3.3. *Eg5 inhibition activates the spindle checkpoint*

The spindle checkpoint is a molecular safeguard that ensures accurate chromosome segregation during mitosis. The checkpoint prevents anaphase onset in the presence of spindle assembly errors or when the chromosomes are not properly/bipolarly attached by spindle microtubules; chromosome segregation is allowed when and only when all the chromosomes are properly attached by microtubules from two opposite spindle poles [7,8]. The defect in bipolar spindle formation caused by dimethylenastron suggested that this agent might activate the spindle checkpoint. We tested this possibility by examining the subcellular localization patterns of three checkpoint proteins, Mad2, Bub1, and BubR1. All of these proteins are essential for spindle checkpoint control in human cells [7,8]. There was no Mad2 signal at kinetochores of chromosomes in normal metaphase cells (Fig. 3A). In contrast, in dimethylenastron-arrested mitotic cells, Mad2 clearly localized at the kinetochores (Fig. 3A). Similarly, we found

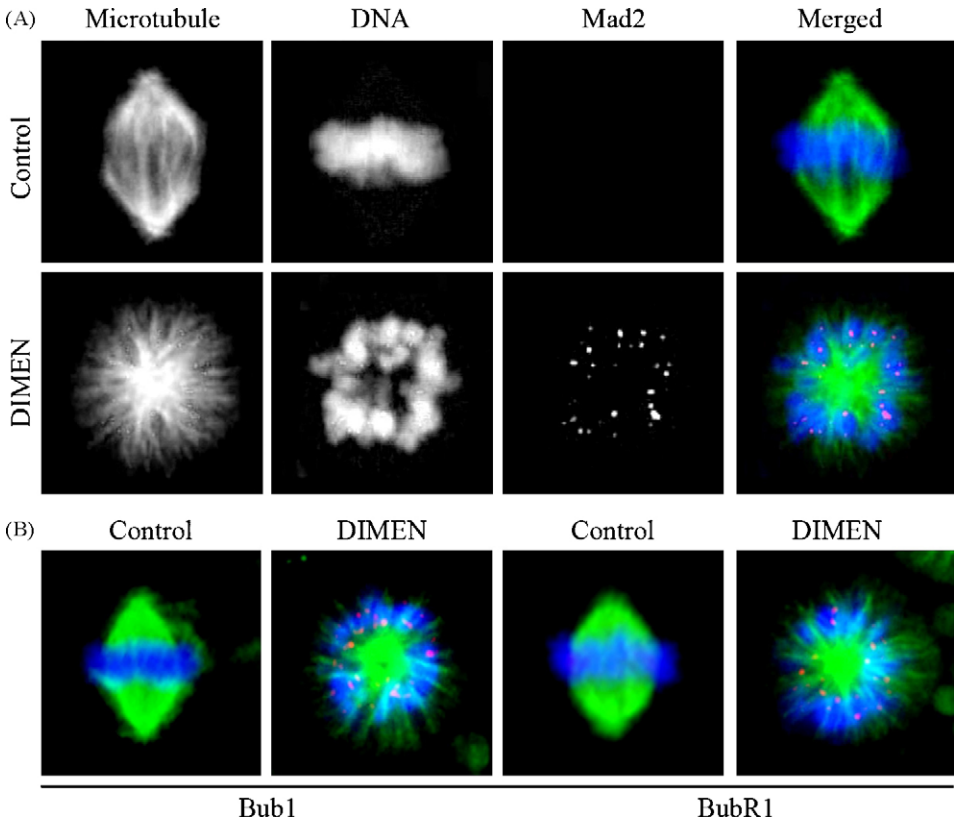

Fig. 3 – Inhibition of Eg5 by dimethylenastron activates the spindle checkpoint. (A) Immunofluorescence images of microtubules (green), DNA (blue), and Mad2 (red) in EPP85 cells treated for 24 h with 0.4 μM dimethylenastron or vehicle (control). (B) Immunofluorescence images of microtubules (green), DNA (blue), and Bub1 or BubR1 (red) in EPP85 cells treated for 24 h with 0.4 μM dimethylenastron or vehicle (control).

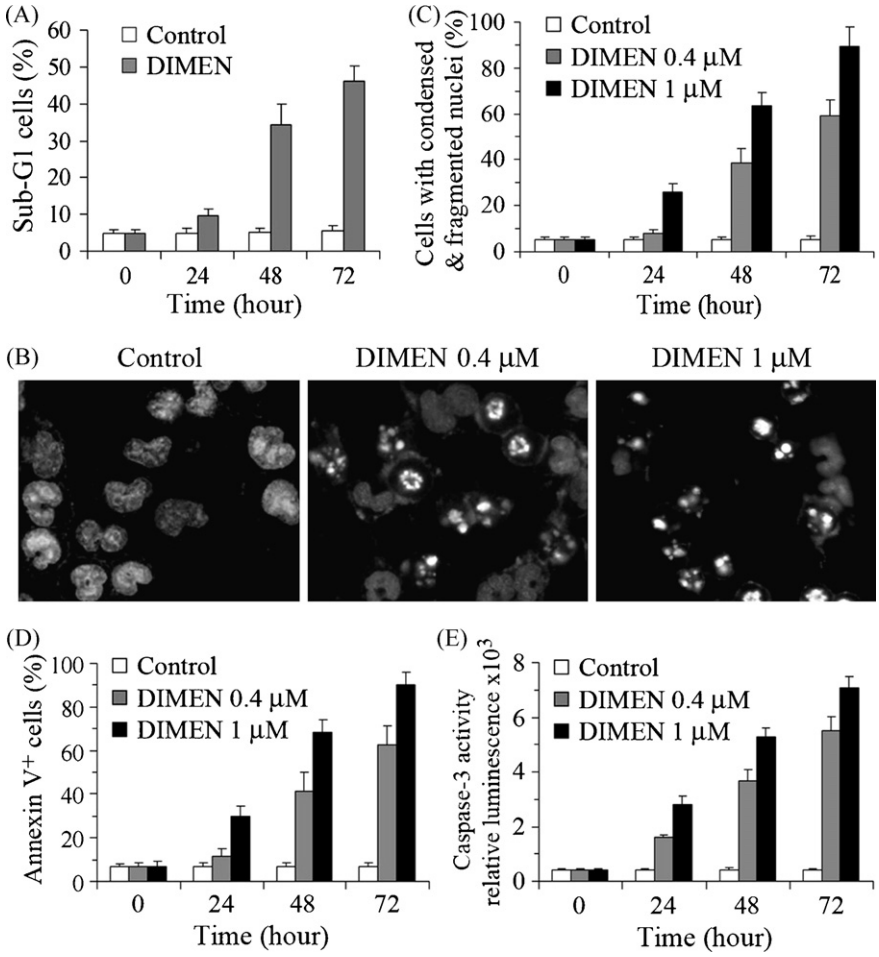

Fig. 4 – Dimethylenastron triggers apoptosis in pancreatic cancer cells. (A) EPP85 cells were treated with 0.4 μM dimethylenastron or vehicle (control) for 0, 24, 48, or 72 h, and the percentage of cells with less than 2N DNA content (sub-G1 population) was quantified by flow cytometric analysis of cellular DNA content. (B) Cells were treated for 48 h with 0.4 or 1 μM dimethylenastron or vehicle (control) and stained with the DNA dye DAPI. The nuclear morphology of cells was then observed under a fluorescence microscope. Apoptotic cells exhibit condensed and fragmented nuclei known as apoptotic bodies. (C) Cells were treated with 0.4 or 1 μM dimethylenastron or vehicle (control) for 0, 24, 48, or 72 h, and the percentage of cells with condensed and fragmented nuclei was quantified by fluorescence microscopy as in (B). More than 300 cells were counted for each group. (D) Cells were treated with 0.4 or 1 μM dimethylenastron or vehicle (control) for 0, 24, 48, or 72 h, and the percentage of apoptotic cells was determined by annexin V staining assay. (E) Cells were treated with 0.4 or 1 μM dimethylenastron or vehicle (control) for 0, 24, 48, or 72 h, and cellular caspase-3 activity was analyzed using the luminogenic substrate Z-DEVD-aminoluciferin.

that Bub1 and BubR1 also resided at the kinetochores in dimethylenastron-arrested cells, although they were absent in normal metaphase cells (Fig. 3B). Thus, dimethylenastron treatment indeed activated the spindle checkpoint in pancreatic cancer cells.

3.4. *Dimethylenastron triggers apoptosis in pancreatic cancer cells*

The morphology of fragmented cells upon prolonged dimethylenastron treatment (Fig. 1B) suggested that this drug might induce apoptosis. We examined this possibility by flow cytometric analysis of cellular DNA content. The percentage of cells with less than 2N DNA content (sub-G1 cell population) was quantified as a measure of apoptosis. Prolonged dimethylenastron treatment was found to significantly increase the proportion of sub-G1 cells (Fig. 4A). The induction of apoptosis by this agent exhibited a time-dependent manner; for example, 36% and 49% of cells underwent apoptosis upon treatment with 0.4 μM dimethylenastron for 48 and 72 h, respectively (Fig. 4A). We also stained the drug-treated cells with the DNA dye DAPI and then examined nuclear morphology to further investigate the incidence of apoptosis. As shown in Fig. 4B, this drug induced the formation of condensed and fragmented nuclei (known as apoptotic bodies) characteristic of apoptosis. The percentage of cells with condensed and fragmented nuclei increased with the time of dimethylenastron treatment (Fig. 4C).

To distinguish apoptosis from other possible causes of cell death, we examined dimethylenastron-treated cells by annexin V staining assay, which reports the loss of phosphatidylserine asymmetry of plasma membrane at the early stage of apoptosis [17]. As shown in Fig. 4D, dimethylenastron increased the percentage of annexin V-positive cells in a time- and concentration-dependent manner. We also examined the activity of caspase-3 in dimethylenastron-treated cells. As the key executioner for apoptosis, caspase-3 is activated by upstream caspases upon apoptotic stimuli, and the activation involves the cleavage of the inactive proenzyme into an active form. The active form can be monitored using a small peptide substrate that becomes luminogenic upon cleavage. As shown in Fig. 4E, we observed a time- and concentration-dependent activation of caspase-3 upon dimethylenastron treatment. Collectively, these results demonstrate that the Eg5 inhibitor dimethylenastron could trigger profound apoptosis in pancreatic cancer cells following mitotic arrest.

3.5. *The spindle checkpoint is a critical determinant of dimethylenastron sensitivity in pancreatic cancer cells*

The next question regarding the mechanism of action of dimethylenastron is whether its activity against pancreatic cancer cells depends on the integrity of the spindle checkpoint, which is frequently compromised in cancer cells [18]. To answer this question, we knocked down the expression of Mad2 and BubR1 in EPP85 cells by specific siRNAs (Fig. 5A). We found that impairment of the spindle checkpoint by Mad2 or BubR1 siRNAs significantly inhibited the ability of dimethy-

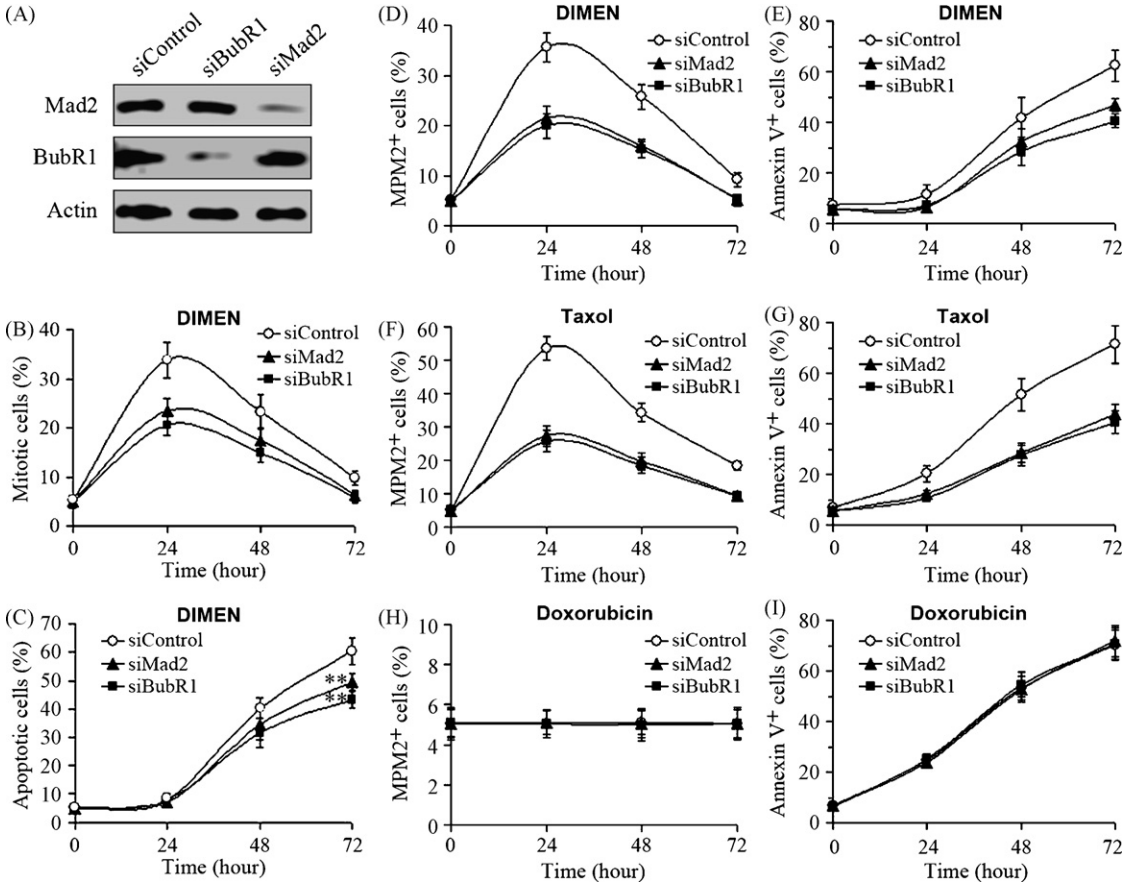

Fig. 5 – Impairment of the spindle checkpoint by decreasing the expression of Mad2 or BubR1 suppresses dimethylenastron-induced mitotic arrest and apoptosis. (A) Western blot analysis of the expression of Mad2, BubR1, and β-actin in EPP85 cells transfected with luciferase (control), Mad2, or BubR1 siRNAs. (B) Cells were transfected with Mad2, BubR1, or control siRNAs for 24 h, and then treated with 0.4 μM dimethylenastron for 0, 24, 48, or 72 h. The percentage of mitotic cells was quantified by immunofluorescence staining of cellular microtubules and DNA. Mitotic cells exhibit condensed chromosomes and monopolar, bipolar, or multipolar spindles. More than 300 cells were counted for each group. (C) Cells were transfected with Mad2, BubR1, or control siRNAs for 24 h, and then treated with 0.4 μM dimethylenastron for 0, 24, 48, or 72 h. The percentage of cells with condensed and fragmented nuclei (apoptotic bodies) was then quantified by fluorescence staining of cellular DNA. More than 300 cells were counted for each group. Values, means of three independent experiments; bars, S.D.; **, $P < 0.01$. (D, F, H) Cells were transfected with Mad2, BubR1, or control siRNAs for 24 h, and then treated with 0.4 μM dimethylenastron (D), 5 nM taxol (F), or 5 nM doxorubicin (H) for 0, 24, 48, or 72 h. The percentage of mitotic cells was quantified by MPM2 antibody staining assay. (E, G, I) Cells were transfected with Mad2, BubR1, or control siRNAs for 24 h, and then treated with 0.4 μM dimethylenastron (E), 5 nM taxol (G), or 5 nM doxorubicin (I) for 0, 24, 48, or 72 h. The percentage of apoptotic cells was then quantified by annexin V staining assay.

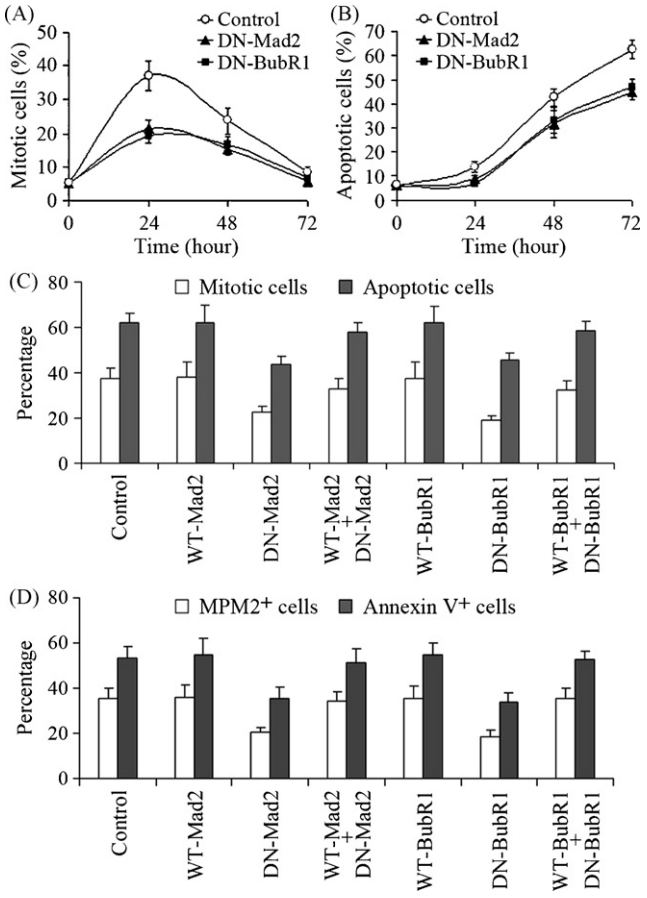

Fig. 6 – Inhibition of dimethylenastron-induced mitotic arrest and apoptosis by the expression of dominant-negative spindle checkpoint proteins. (A) Cells were treated with dominant-negative Mad2 (DN-Mad2), dominant-negative BubR1 (DN-BubR1), or control (β-galactosidase) adenoviruses for 24 h, and then with 0.4 μM dimethylenastron for 0, 24, 48, or 72 h. The percentage of mitotic cells was quantified by immunofluorescence staining of cellular microtubules and DNA. (B) Cells were treated with DN-Mad2, DN-BubR1, or control adenoviruses for 24 h, and then with 0.4 μM dimethylenastron for 0, 24, 48, or 72 h. The percentage of cells with condensed and fragmented nuclei was then quantified by fluorescence staining of cellular DNA. (C) Cells were treated with the indicated adenoviruses for 24 h, and then treated with 0.4 μM dimethylenastron for 24 h to quantify mitotic cells as in (A), or treated for 48 h to quantify apoptotic cells as in (B). (D) Cells were treated with the indicated adenoviruses for 24 h, and then treated with 0.4 μM dimethylenastron for 24 h to quantify mitotic cells by MPM2 antibody staining assay, or treated for 48 h to quantify apoptotic cells by annexin V staining assay.

lenastron to arrest cells at mitosis (Fig. 5B and D), demonstrating a critical role for the spindle checkpoint in mediating dimethylenastron-induced mitotic arrest. Moreover, knockdown of Mad2 or BubR1 significantly prevented cells from apoptosis induced by dimethylenastron (Fig. 5C and E). We observed the same phenomenon using different concentrations of dimethylenastron ranging from 0.1 to 1 μM (Supplementary Figure 1). In addition, we found that impairment of the spindle checkpoint by Mad2 and BubR1 siRNAs also inhibited the ability of taxol to arrest mitosis and to induce apoptosis (Fig. 5F and G). However, Mad2 and BubR1 siRNAs did not affect the percentage of apoptosis induced by doxorubicin, a DNA-binding drug that does not arrest mitosis (Fig. 5H and I). Together, these data demonstrate that the

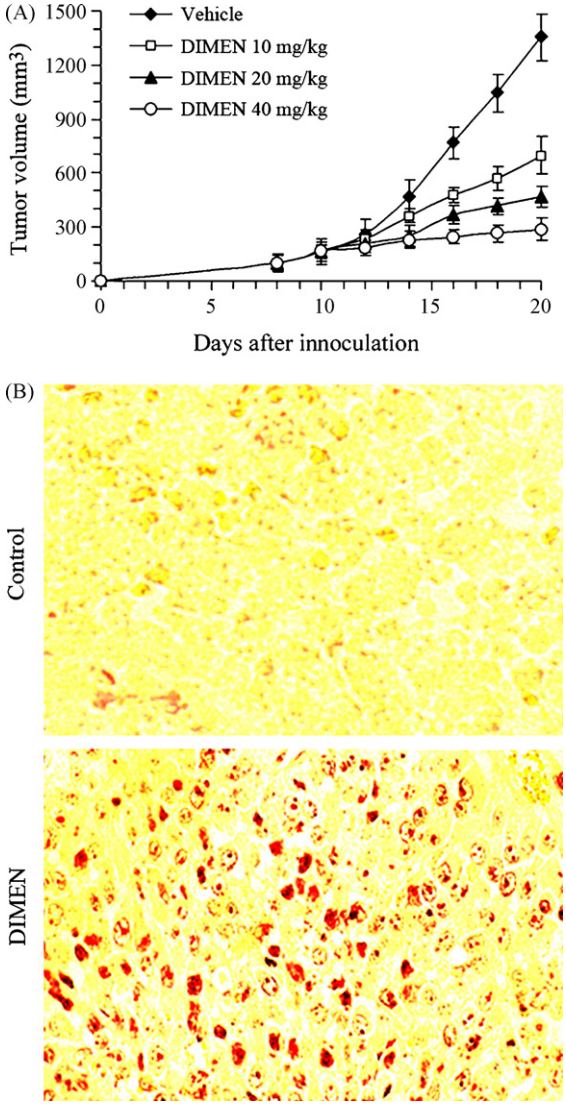

Fig. 7 – Dimethylenastron is effective against tumor xenografts of human pancreatic cancer. (A) Palpable tumors were established in athymic mice after subcutaneous injection of EPP85 cells, and mice were then treated intravenously with 10, 20, or 40 mg/kg dimethylenastron or equal volume of vehicle. Each treatment group comprised 8 mice. Tumor volume was measured every 2 days and is shown as mm^3 ± standard deviation. (B) Dimethylenastron inhibits tumor growth by triggering apoptosis. Shown are representative TUNEL-stained micrographs of tumor sections from vehicle control-treated and 40 mg/kg dimethylenastron-treated mice.

spindle checkpoint is a critical determinant of dimethylenastron sensitivity in pancreatic cancer cells.

To further examine the effect of the spindle checkpoint on dimethylenastron sensitivity, we inhibited the function of Mad2 and BubR1 by using specific dominant-negative adenoviruses. Similar to the results revealed by siRNAs, impairment of the spindle checkpoint by the dominant-negative adenoviruses also inhibited the activity of dimethylenastron to induce mitotic arrest and apoptosis (Fig. 6A and B). Furthermore, treatment of cells with excessive wild-type Mad2 or BubR1 adenoviruses was able to largely restore the mitotic arrest and apoptosis induced by dimethylenastron (Fig. 6C and D). These results thus support the conclusion that the spindle checkpoint regulates Eg5 inhibitor sensitivity.

3.6. *Dimethylenastron is effective against tumor xenografts of human pancreatic cancer*

We next investigated whether dimethylenastron was effective against human pancreatic tumors implanted subcutaneously in nude mice. When tumor xenografts were palpable with tumor size of about 100 mm^3, we grouped the mice randomly into four groups of 8 animals each. The mice were then treated intravenously with 10, 20, or 40 mg/kg dimethylenastron or equal volume of vehicle. As shown in Fig. 7A, dimethylenastron treatment significantly reduced tumor volume in EPP85 xenografts in a dose-dependent manner. On day 20 of treatment, 40 mg/kg dimethylenastron reduced tumor volume by 78.8% as compared to the vehicle control (from 1355 to 287 mm^3, average tumor volume). Dimethylenastron treatment did not cause any apparent body weight loss in mice (data not shown). We next asked whether dimethylenastron caused tumor regression in the xenografts by triggering apoptosis. Consistent with our results achieved from annexin V staining, caspase-3 activation, and other apoptotic assays in cultured cells, we observed a widespread staining of TUNEL-positive cells in the regressed tumors of dimethylenastron-treated EPP85 tumor xenografts (Fig. 7B). This result indicates that dimethylenastron causes tumor regression by inducing apoptosis.

4. Discussion

Pancreatic cancer is a highly malignant disease with a grim prognosis. The mortality rate of this disease is similar to its incidence rate; most patients die within a year of diagnosis [1]. The poor clinical outcome of pancreatic cancer is mainly attributed to the delay in diagnosis, the propensity of this cancer to rapidly metastasize, and its resistance to currently approved drugs [2,3]. Chemotherapeutic management of this disease has rather limited efficacy and does not provide convincing results. Gemcitabine has been the standard agent over the past decade for the treatment of advanced pancreatic cancer, and it leads to modest clinical benefit in a small proportion of patients [4]. Gemcitabine in combination with erlotinib, a drug targeting the epidermal growth factor receptor, was recently approved in the United States for the treatment of advanced disease. However, the gemcitabine/erlotinib combination only slightly improves patient survival over gemcitabine alone [4], underlying the paramount importance to characterize additional targets. In this study, we demonstrate that dimethylenastron, a specific Eg5 inhibitor, effectively inhibits cell proliferation and induces apoptosis in pancreatic cancer cells and tumor xenografts. This finding indicates Eg5 as a potential target for the treatment of pancreatic cancer.

The data presented in this study also provide mechanistic insights into the anti-proliferative activity of dimethylenastron. Immunofluorescence microscopy, flow cytometry, and MPM2 antibody staining assays reveal that the Eg5 inhibitor prevents cell proliferation by arresting cell-cycle progression at mitosis. In addition, our data show that the mitotic arrest induced by dimethylenastron results from its interference with bipolar spindle formation and activation of the spindle checkpoint. The monopolar spindle phenotype induced by dimethylenastron is similar to that observed when cells are treated with other Eg5 inhibitors [19–22] or injected with Eg5 antibodies [23,24], and supports a critical role for Eg5 in bipolar spindle assembly. The spindle checkpoint halts mitotic progression primarily through the checkpoint proteins Mad2, Bub1, and BubR1, in the presence of spindle assembly errors or when the chromosomes are not properly/bipolarly attached by spindle microtubules. Unattached or improperly attached kinetochores are known to act as catalytic sites for the activation of these checkpoint proteins, which in turn prevent anaphase onset by inhibiting the anaphase promoting complex [7,8]. Given the severe spindle assembly defects and monopolar spindle phenotype in dimethylenastron-treated cells, apparently the chromosomes in these cells are not properly/bipolarly attached by spindle microtubules. This is likely to be the cause for the localization of Mad2, Bub1, and BubR1 to the kinetochores of chromosomes.

Our data show that impairment of the spindle checkpoint by knockdown of Mad2, Bub1, or BubR1 expression or by suppression of their function significantly reduces the mitotic arrest induced by dimethylenastron, further supporting the conclusion that the Eg5 inhibitor-induced mitotic arrest is due to spindle checkpoint activation. Importantly, dimethylenastron-induced apoptosis is also significantly compromised following spindle checkpoint impairment. In addition, a functional spindle checkpoint is also required for mitotic arrest and apoptosis induced by the microtubule-binding antimitotic drug taxol. In contrast, apoptosis induced by doxorubicin, a DNA-binding drug not arresting mitosis, is not affected by the spindle checkpoint status. These findings suggest that mitotic arrest and apoptosis caused by anti-mitotic agents, including Eg5 inhibitors and microtubule inhibitors, are two intimately related events. It is possible that the spindle checkpoint per se has pro-apoptotic activity, but the pro-apoptotic activity is normally inhibited by anti-apoptotic mitotic proteins such as survivin. Treatment with Eg5 inhibitors may cause mitotic slippage after a sustained mitotic arrest, leading to the inactivation of anti-apoptotic proteins and thereby inducing apoptosis. This hypothesis is supported by the finding that the spindle checkpoint protein BubR1 possesses pro-apoptotic activity [25]. In this context, it is not difficult to understand how the loss of spindle checkpoint proteins leads to resistance to dimethylenastron; loss of the checkpoint proteins may simply shift the balance between pro-apoptotic and anti-apoptotic components

toward the anti-apoptotic side and thereby confers resistance to Eg5 inhibitors.

Our finding that Eg5 inhibitor sensitivity in pancreatic cancer cells depends on a functional spindle checkpoint suggests that spindle checkpoint proteins may serve as additional targets for chemotherapy to improve activity of the drug and prevent resistance. On the other hand, our data implicate that the spindle checkpoint is a potential biomarker for predicting the efficacy of Eg5-targeted therapies. The identification of successful biomarkers represents an important step towards the individualization of pancreatic cancer therapy [26,27]. Our results suggest that patients with spindle checkpoint-competent tumors would more likely benefit from Eg5 inhibitor-based treatment, compared with patients with spindle checkpoint-defective tumors.

Acknowledgements

We would like to thank Dr. Harish C. Joshi for providing reagents. This work was supported in part by grants from the National Basic Research Program of China (2007CB914301), the Tianjin Natural Science Foundation (07JCZDJC03000), the Ph.D. Program Foundation (20060055008), and the New Century Excellent Talents Program (NCET-06-0217), Ministry of Education, China.

Appendix A. Supplementary data

Supplementary data associated with this article can be found, in the online version, at doi:10.1016/j.bcp.2008.04.018.

REFERENCES

[1] Jemal A, Siegel R, Ward E, Murray T, Xu J, Smigal C, et al. Cancer statistics. CA Cancer J Clin 2006;56:106–30.
[2] Hezel AF, Kimmelman AC, Stanger BZ, Bardeesy N, Depinho RA. Genetics and biology of pancreatic ductal adenocarcinoma. Genes Dev 2006;20:1218–49.
[3] Ghaneh P, Costello E, Neoptolemos JP. Biology and management of pancreatic cancer. Gut 2007;56:1134–52.
[4] Kindler HL. Pancreatic cancer: an update. Curr Oncol Rep 2007;9:170–6.
[5] Van Laethem JL, Marechal R. Emerging drugs for the treatment of pancreatic cancer. Expert Opin Emerg Drugs 2007;12:301–11.
[6] Gartner M, Sunder-Plassmann N, Seiler J, Utz M, Vernos I, Surrey T, et al. Development and biological evaluation of potent and specific inhibitors of mitotic kinesin Eg5. Chembiochem 2005;6:1173–7.
[7] May KM, Hardwick KG. The spindle checkpoint. J Cell Sci 2006;119:4139–42.
[8] Musacchio A, Salmon ED. The spindle-assembly checkpoint in space and time. Nat Rev Mol Cell Biol 2007;8:379–93.
[9] Sudo T, Nitta M, Saya H, Ueno NT. Dependence of paclitaxel sensitivity on a functional spindle assembly checkpoint. Cancer Res 2004;64:2502–8.
[10] Zhou J, O'Brate A, Zelnak A, Giannakakou P. Survivin deregulation in beta-tubulin mutant ovarian cancer cells underlies their compromised mitotic response to taxol. Cancer Res 2004;64:8708–14.
[11] Zhou J, Liu M, Aneja R, Chandra R, Lage H, Joshi HC. Reversal of P-glycoprotein-mediated multidrug resistance in cancer cells by the c-Jun NH2-terminal kinase. Cancer Res 2006;66:445–52.
[12] Liu M, Aneja R, Liu C, Sun L, Gao J, Wang H, et al. Inhibition of the mitotic kinesin Eg5 up-regulates Hsp70 through the phosphatidylinositol 3-kinase/Akt pathway in multiple myeloma cells. J Biol Chem 2006;281:18090–7.
[13] Xuan C, Qiao W, Gao J, Liu M, Zhang X, Cao Y, et al. Regulation of microtubule assembly and stability by the transactivator of transcription protein of Jembrana disease virus. J Biol Chem 2007;282:28800–6.
[14] Duhl DM, Renhowe PA. Inhibitors of kinesin motor proteins—research and clinical progress. Curr Opin Drug Discov Devel 2005;8:431–6.
[15] Vichai V, Kirtikara K. Sulforhodamine B colorimetric assay for cytotoxicity screening. Nat Protoc 2006;1:1112–6.
[16] Davis FM, Tsao TY, Fowler SK, Rao PN. Monoclonal antibodies to mitotic cells. Proc Natl Acad Sci USA 1983;80:2926–30.
[17] van Engeland M, Nieland LJ, Ramaekers FC, Schutte B, Reutelingsperger CP. Annexin V-affinity assay: a review on an apoptosis detection system based on phosphatidylserine exposure. Cytometry 1998;31:1–9.
[18] Kops GJ, Weaver BA, Cleveland DW. On the road to cancer: aneuploidy and the mitotic checkpoint. Nat Rev Cancer 2005;5:773–85.
[19] Kapoor TM, Mayer TU, Coughlin ML, Mitchison TJ. Probing spindle assembly mechanisms with monastrol, a small molecule inhibitor of the mitotic kinesin, Eg5. J Cell Biol 2000;150:975–88.
[20] Hotha S, Yarrow JC, Yang JG, Garrett S, Renduchintala KV, Mayer TU, et al. HR22C16: a potent small-molecule probe for the dynamics of cell division. Angew Chem Int Ed Engl 2003;42:2379–82.
[21] Sakowicz R, Finer JT, Beraud C, Crompton A, Lewis E, Fritsch A, et al. Antitumor activity of a kinesin inhibitor. Cancer Res 2004;64:3276–80.
[22] Tao W, South VJ, Zhang Y, Davide JP, Farrell L, Kohl NE, et al. Induction of apoptosis by an inhibitor of the mitotic kinesin KSP requires both activation of the spindle assembly checkpoint and mitotic slippage. Cancer Cell 2005;8:49–59.
[23] Sawin KE, LeGuellec K, Philippe M, Mitchison TJ. Mitotic spindle organization by a plus-end-directed microtubule motor. Nature 1992;359:540–3.
[24] Blangy A, Lane HA, d'Herin P, Harper M, Kress M, Nigg EA. Phosphorylation by p34cdc2 regulates spindle association of human Eg5, a kinesin-related motor essential for bipolar spindle formation in vivo. Cell 1995;83:1159–69.
[25] Shin HJ, Baek KH, Jeon AH, Park MT, Lee SJ, Kang CM, et al. Dual roles of human BubR1, a mitotic checkpoint kinase, in the monitoring of chromosomal instability. Cancer Cell 2003;4:483–97.
[26] Jimeno A, Hidalgo M. Molecular biomarkers: their increasing role in the diagnosis, characterization, and therapy guidance in pancreatic cancer. Mol Cancer Ther 2006;5:787–96.
[27] Giovannetti E, Mey V, Nannizzi S, Pasqualetti G, Del Tacca M, Danesi R. Pharmacogenetics of anticancer drug sensitivity in pancreatic cancer. Mol Cancer Ther 2006;5:1387–95.